Journal of Catalysis **211,** 422–433 (2002)
doi:10.1006/jcat.2002.3749

An Investigation of the Effects of Water on Rate and Selectivity for the Fischer–Tropsch Synthesis on Cobalt-Based Catalysts

Sundaram Krishnamoorthy,[1] Mai Tu, Manuel P. Ojeda,[2] Dario Pinna,[3] and Enrique Iglesia[4]

Department of Chemical Engineering, University of California at Berkeley, Berkeley, California 94720

Received March 26, 2002; revised July 2, 2002; accepted July 15, 2002

Water, the primary oxygen-containing product in Co-catalyzed Fischer–Tropsch synthesis (FTS), increases CO conversion rates and the selectivity to olefins and to C_{5+} products. These marked rate and selectivity enhancements can reflect changes in the density or reactivity of the active Co surface atoms available during FTS. Kinetic isotope effects and *in situ* infrared spectroscopy were used to probe possible mechanisms for these water effects. Kinetic isotope effects (r_H/r_D) measured from CO/H_2 and CO/D_2 were less than unity for both CO conversion and C_{5+} formation rates, suggesting that hydrogen adsorption–desorption thermodynamics and C–H bond formation are involved in kinetically relevant FTS steps. The presence of varying amounts of water (H_2O or D_2O) did not influence the measured kinetic isotope values, even though water in concentration range led to marked changes in FTS rate and selectivity. Thus, the isotopic identity of the water molecules does not influence the rate of kinetically relevant steps, the identity of which appears to remain unchanged by the presence of water. No new pathways are apparently introduced by the presence of water in H_2/CO reactant streams. The intensity and vibrational frequency of adsorbed CO bands were also not influenced by the concentration of water in the reactant stream. These *in situ* infrared spectroscopic studies showed that water does not influence the density or structure of adsorbed CO intermediates or the number of exposed Co atoms, which bind CO at near-monolayer coverages during Fischer–Tropsch synthesis reactions. These spectroscopic studies also suggest that neither CO transport restrictions nor their removal via the formation of water-rich intrapellet liquids at high water concentrations are responsible for the observed effects of water. These studies are silent about a possible effect of water on the concentration of reactive carbon species, which may be present as minority but kinetically relevant intermediates during FTS.

INTRODUCTION

Cobalt surface atoms show high activity and C_{5+} selectivity in Fischer–Tropsch synthesis (FTS), which currently provides the most economic path for the synthesis of liquid fuels from natural gas (1–4). Oxygen atoms in CO coreactants are predominately removed as H_2O on Co-based catalysts. Commercial FTS practice requires that Co catalysts withstand long-term use at high CO conversions, during which water concentrations approach saturation levels and may even condense within catalyst support pores. The effects of water on the extent of oxidation of Co crystallites have been recently addressed (5). Here, we focus on the kinetic effects of water on FTS rates and selectivities.

H_2O molecules, whether indigenous or added to H_2/CO reactants, increase FTS rates on Co/SiO_2 (6, 7), Co/TiO_2 (6, 7), and Co–Mg–Th–Aerosil (8), but they inhibit reaction rates on Co supported on Mn and Al oxides (5, 9, 10). H_2O increases C_{5+} selectivity and decreases CH_4 selectivity on all these Co-based catalysts (6–8, 11, 12). X-ray photoelectron spectra (5) have detected the oxidation of surface Co atoms in Co/Al_2O_3 samples exposed to high H_2O concentrations during FTS. Bulk oxidation of Co metal to CoO or Co_3O_4 is not thermodynamically favored at typical FTS conditions, but metal–oxygen bonds at metal surfaces are stronger than in bulk oxides, making the oxidation of Co surfaces possible even when bulk oxidation is unfavorable. Also, small metal clusters strongly interacting with oxide supports tend to be more prone to oxidation than larger bulk-like Co crystallites because of their extensive contact with the oxide support. Isotopic transients during steady-state FTS reactions have shown that high water concentrations decrease the number of exposed Co atoms (13, 14). These transient studies did not detect any changes, however, in the intrinsic activity of exposed surface atoms with changes in H_2O concentration.

H_2O effects on the rate and C_{5+} selectivity of FTS reactions on Co catalysts supported on TiO_2 and SiO_2 could reflect CO transport restrictions, which can be alleviated by the higher CO diffusion rates through an intraparticle water-rich liquid phase stabilized by capillary effects and favored at high H_2O concentrations (7). The influence of

[1] Current address: W. R. Grace & Co., 7500 Grace Drive, Columbia, MD 21044.

[2] Current address: Instituto de Catalisis y Petroleoquimica (CSIC), 28049 Madrid, Spain.

[3] Current address: Department of Industrial Chemistry and Chemical Engineering "Giulio Natta," Politecnico di Milano, Piazza Leonardo da Vinci, 2-20133 Milano, Italy.

[4] To whom correspondence should be addressed. E-mail: iglesia@cchem.berkeley.edu.

0021-9517/02 $35.00

the support pore structure on the magnitude of these water effects and the well-documented effects of intrapellet transport restrictions on FTS rates and selectivity provide indirect support for this proposal (7). Larger pores would require higher H_2O concentrations in order to form a water-rich phase, while smaller pores would stabilize such a phase even at low water concentrations (7). TiO_x overlayers can form during prereduction on TiO_2-supported Co catalysts; these overlayers may be removed in the more oxidizing environments prevalent at high H_2O concentrations (15). In the latter case, the beneficial effects of water may arise from the removal of TiO_x overlayers from Co metal surfaces at high water concentrations. Such overlayers do not form on silica supports; yet, some Co/SiO_2 catalysts, and even unsupported Co powders (6), have shown strong effects of water on FTS rate and selectivity.

A few reported FTS kinetic rate expressions contain water concentration terms, suggesting a possible role of water in kinetically relevant elementary steps (16, 17). These water effects, however, cannot be attributed unequivocally to the chemical involvement of water in chain growth reaction pathways; they may reflect instead changes in the local concentrations of reactants and products (controlled by diffusional constraints) or a change in the accessibility of Co surface metal atoms (caused by the removal of reduced oxide overlayers or of unreactive carbonaceous deposits). Here, we attempt to discern these potential roles of H_2O in controlling the accessibility and chemical properties of active Co surface metal atoms.

In this study, chemical effects of H_2O on FTS reaction pathways are probed by measuring (H/D) kinetic isotope effects (KIE) at various water concentrations. The availability of Co surface atoms during FTS was examined using *in situ* FTIR spectroscopy, which measures the number and type of CO binding sites as H_2O concentrations change during FTS. *In situ* infrared spectra of adsorbed CO reactants during FTS have been reported on Ru, Co, and Fe, but at low pressures, high temperatures, or low CO conversions, all of which lead to methane as the predominant reaction product (18–22). Stretching modes for linearly adsorbed CO, $-CH_2$, and $-CH_3$ groups, as well as for surface formates, have been reported on Ru/Al_2O_3 (18). Bridged CO adsorbed species were also detected on Ru/SiO_2 (19). The $-CH_2$ and $-CH_3$ bands arise from growing chains (19, 20) and from hydrocarbons physisorbed or condensed within catalyst pores. These adsorbed species have also been reported in less detailed infrared studies on Co/Al_2O_3 catalysts (21, 22).

These previous studies did not address the effects of reaction conditions, and specifically of H_2O concentration, on the surface coverage and vibrational frequency of adsorbed species. Co surfaces are predominately covered by adsorbed CO during FTS (23). Therefore, the intensity of the CO infrared bands measured during reaction can be used to estimate the number of Co surface atoms able to chemisorb and activate CO *during* Fischer–Tropsch synthesis reactions.

We present here kinetic isotope effects and FTS rates and selectivities as a function of H_2O concentration, as well as *in situ* infrared spectra collected during FTS, on Co/SiO_2 catalysts. These studies attempt to elucidate the possible effects of water on the fraction of the Co surface atoms available for FTS reactions, on their oxidation state, and on the identity and rate of kinetically relevant elementary steps in the Fischer–Tropsch synthesis.

EXPERIMENTAL METHODS

Catalyst Synthesis and Characterization

Co/SiO_2 catalysts with 12.7 and 21.9 wt% Co were prepared by incipient wetness impregnation of SiO_2 (PQ Corp. CS-2133; treated in dry air at 673 K for 3 h) with the required volume of aqueous Co nitrate solutions (Aldrich, 98%). The impregnated support was dried at 333 K in ambient air for 24 h and treated in flowing H_2 (1.2×10^4 $cm^3/h \cdot g\text{-cat}$) by increasing the temperature from 293 to 423 K at 0.17 K/s and from 423 to 623 K at 8.3×10^{-3} K/s, and then holding at 623 K for 1 h. These samples were passivated in flowing 1% O_2/He at room temperature before exposure to ambient air. The Co dispersion was measured using H_2 chemisorption (AutoSorb-1, Quantachrome) at 373 K, after passivated samples were re-reduced in H_2 at 598 K, evacuated to $<10^{-3}$ Pa at 598 K, and cooled to 373 K (24). A 1 : 1 H/Co titration stoichiometry was used to calculate the cobalt dispersion (24). The measured Co metal dispersions were 5.8 and 4.6% for the 12.7 and 21.9 wt% Co/SiO_2 catalysts, respectively.

Fischer–Tropsch Synthesis Rates and Product Selectivities

Fischer–Tropsch synthesis rates and selectivities were measured using an isothermal packed-bed reactor with plug-flow hydrodynamics. The details of the reactor and of the analytical system have been reported elsewhere (25). Co/SiO_2 (12.7 wt%, 1.75 g 100- to 180-μm particles) diluted with SiO_2 (2.8 g, 100- to 180-μm particles) was used in these measurements. The catalyst was reduced in H_2 (12×10^3 $cm^3/h \cdot g\text{-cat}$) within the reactor by heating to 598 K at 0.17 K/s and holding for 1 h. FTS reactions were carried out at 473 K using synthesis gas (Praxair, 62% H_2, 31% CO, 7% N_2 internal standard) at two different pressures (0.5 and 2.0 MPa). The concentrations of CO, CO_2, and all hydrocarbon products (C_1–C_{15}) were measured using online gas chromatography (25). Water was added to the synthesis gas reactant stream using an ISCO 440D Series pump and all transfer lines were maintained at 410 K or higher in order to prevent condensation. FTS rates and selectivity data were also measured on 21.9 wt% Co/SiO_2, but the data are not

reported here, because the observed trends were essentially identical to those obtained on 12.7 wt% Co/SiO_2.

Kinetic Isotope Effect Measurements

H_2/D_2 isotope effects were measured using $H_2/CO/N_2$ (62%/31%/7%) and $D_2/CO/N_2$ (62%/31%/7%) reactant mixtures. The reactants, H_2 (Matheson, 99.999%), D_2 (Cambridge Isotope Laboratories, 99.8%), and CO/N_2 (Matheson, 81.5% CO/18.5% N_2), were introduced separately and mixed, before entering the reactor. Co/SiO_2 (21.9 wt%, 1.0 g, 100–180 μm) diluted with SiO_2 (3.2 g, 100–180 μm) was reduced in H_2 before FTS reaction measurements, using the procedures described above. Reactant and product concentrations were measured using previously reported chromatographic protocols (25). Similar detector response factors were used for deuterated and undeuterated hydrocarbons.

In Situ Infrared Spectra Measurements

In situ infrared spectra were measured using a Mattson RS-1000 Spectrometer in the transmission mode with a resolution of 2 cm^{-1}. A stainless-steel cell with CaF_2 windows was used in all experiments (Fig. 1). The catalyst sample consisted of a thin wafer held in the beam path. The gas-phase optical path was minimized by using packed CaF_2 disks on each side of the pellet; these disks also minimized the dead volume within the cell. The temperature was held constant using an external resistive heater surrounding the cell. The CaF_2 windows were kept to 353 K using a continuous flow of water. The sample temperature was monitored using a *K*-type thermocouple (Omega, 0.08-cm diameter, 10-cm length) held within 1 mm of the center of the sample wafer.

Sample disks (20×1 mm) were prepared by pressing a mixture of Co/SiO_2 (0.07 g) and Al_2O_3 (Alon, 0.03 g) at ~100 MPa. These wafers were first treated in O_2/He (3.6×10^3 cm^3/h) at 623 K for 0.5 h in order to remove any species adsorbed during exposure to ambient air. The cell was flushed briefly with He at 623 K and the sample reduced in H_2 (1 cm^3/s) at 623 K for 2 h. The temperature of the cell was then decreased to 473 K in H_2 and a background spectrum was collected. Synthesis gas ($H_2:CO = 2:1$, 4.8×10^3 cm^3/h) was introduced and the pressure was increased to 0.5 MPa to match the conditions of the catalytic reactor measurements. Spectra were collected at 453 and 473 K while the samples were contacted with synthesis gas containing varying H_2O concentrations. Water was introduced using the same equipment and procedures as for the catalytic reactor. Heating and cooling cycles were carried out at 0.082 K/s in order to prevent damage to the CaF_2 windows. The infrared spectra were corrected for absorption by CO in the gas phase by subtracting the spectrum obtained without a wafer at each temperature.

RESULTS AND DISCUSSION

Effects of Water on Fischer–Tropsch Synthesis Rate and Selectivity

Fischer–Tropsch synthesis rates and selectivities were first measured at 473 K and 2 MPa on 12.7 wt% Co/SiO_2. CO

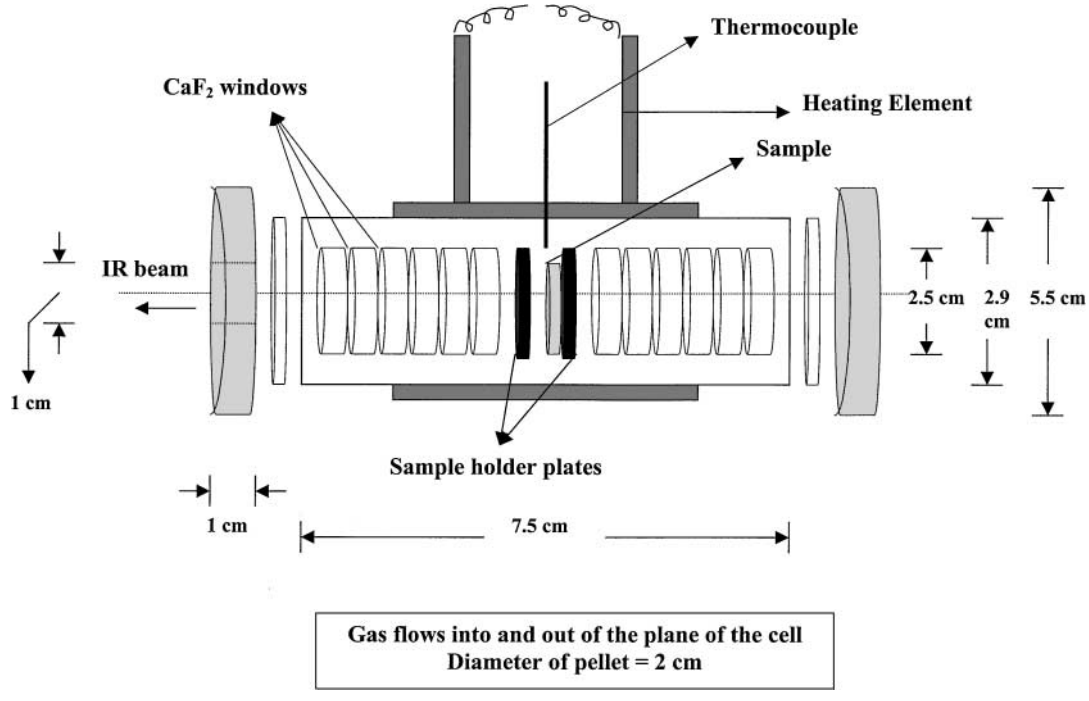

FIG. 1. Schematic representation of the FTIR cell.

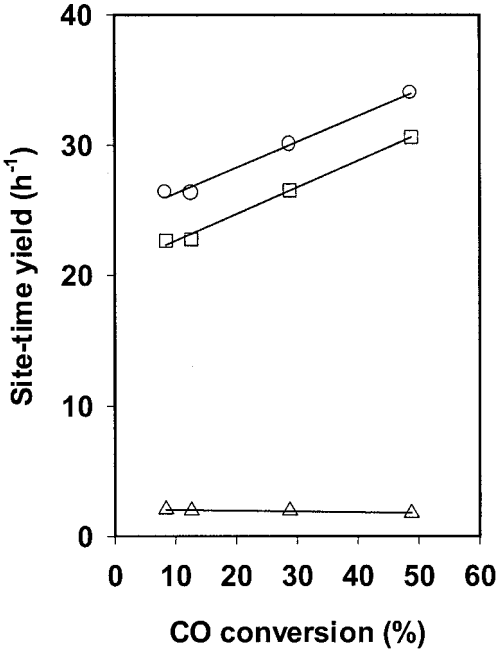

FIG. 2. CO consumption rate (○), C_{5+} formation rate (□), and CH_4 formation rate (△) as a function of CO conversion on 12.7 wt% Co/SiO_2 catalyst at 473 K, 2 MPa, $H_2/CO = 2$. CO conversion was varied by changing the synthesis gas space velocity; site-time yields defined as molar rates per surface Co atom measured by H_2 chemisorption.

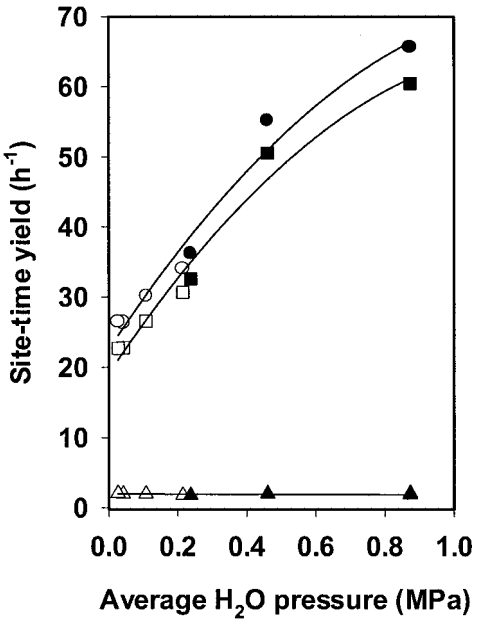

FIG. 3. CO consumption rate (○, ●), C_{5+} formation rate (□, ■), and CH_4 formation rate (△, ▲) as a function of the average water partial pressure on 12.7 wt% Co/SiO_2 catalyst at 473 K, 2 MPa, $H_2/CO = 2$. (Open symbols) Space velocity runs; (filled symbols) water-addition runs.

conversion rates (expressed as site-time yields, i.e., molar CO conversion rate per exposed Co atom) increased with increasing CO conversion, which was varied by decreasing the reactant space velocity (Fig. 2). This unusual behavior suggests that one of the reaction products increases reaction rates, because the depletion of reactants with increasing conversion would otherwise lead to lower rates. Also, C_{5+} formation rates increased with increasing residence time, while CH_4 formation rates were essentially unaffected by changes in residence time and CO conversion. The proposal that one of the reaction products is responsible for these rate enhancements was confirmed by adding H_2O to the synthesis gas reactants at high space velocities (0.86 $cm^3/(g \cdot s)$) and low CO conversions (8.4%). CO conversion and CH_4 and C_{5+} formation rates are shown in Fig. 3 as a function of the average H_2O partial pressure within the catalyst bed for both H_2O addition (open symbols) and space velocity (solid symbols) experiments. The results of these two experiments fall into a single curve, with H_2O concentration as the only relevant variable, irrespective of whether the H_2O concentration was changed by adding H_2O or by varying the CO conversion through changes in residence time. CO conversion and C_{5+} formation rates increased monotonically with increasing H_2O concentration and reached almost constant values at about 0.8 MPa H_2O. These H_2O effects were entirely reversible upon cycling from high to low H_2O concentrations. CH_4 formation rates were not strongly influenced by changes in H_2O concentration (Figs. 2 and 3).

CH_4 and C_{5+} selectivities measured on 12.7 wt% Co/SiO_2 are shown in Fig. 4, 1-pentene/*n*-pentane ratios are shown in Fig. 5 at 473 K and 2.0 MPa, and more detailed results are included in Table 1. Water, whether indigenous or externally

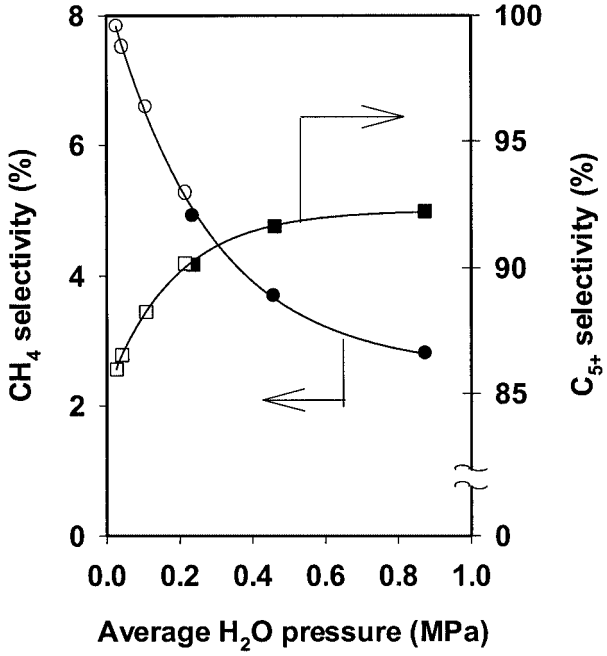

FIG. 4. CH_4 selectivities (○, ●) and C_{5+} selectivities (□, ■) as a function of the average water partial pressure on 12.7 wt% Co/SiO_2 catalyst at 473 K, 2.0 MPa, $H_2/CO = 2$. (Open symbols) Space velocity runs; (filled symbols) water-addition runs.

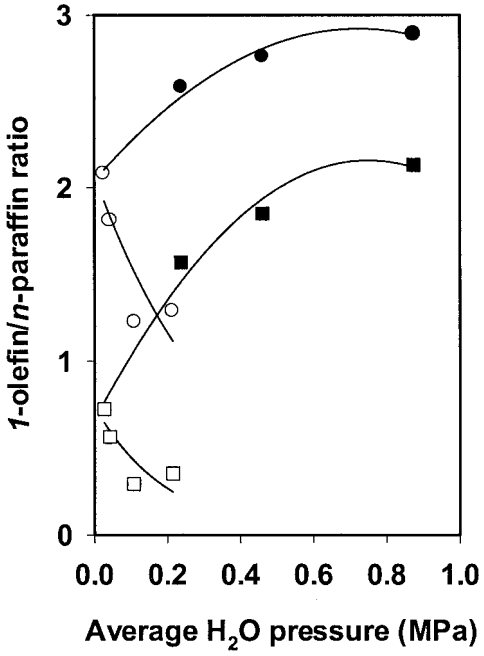

FIG. 5. 1-Pentene/*n*-pentane ratios (○, ●) and 1-octene/*n*-octane ratios (□, ■) as a function of the average water partial pressure on 12.7% Co/SiO_2 catalyst at 473 K, 2.0 MPa, $H_2/CO = 2$. (Open symbols) Space velocity runs; (filled symbols) water-addition runs.

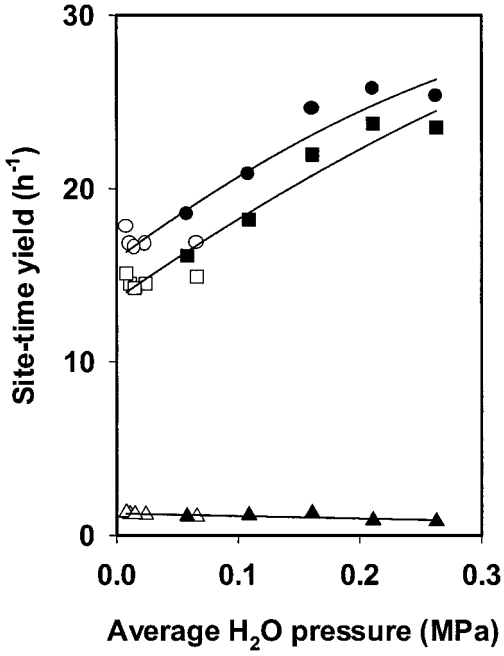

FIG. 6. CO consumption rate (○, ●), C_{5+} formation rate (□, ■), and CH_4 formation rate (△, ▲) as a function of the average water partial pressure on 12.7 wt% Co/SiO_2 catalyst at 473 K, 0.5 MPa, $H_2/CO = 2$. (Open symbols) Space velocity runs; (filled symbols) water-addition runs.

added, increased the average molecular weight of FTS reaction products. Also, the olefin content in these products (e.g., 1-pentene/*n*-pentane ratio) increased when water was added at a given space velocity, as a result of the combined contributions of a much lower rate of chain termination via hydrogen addition and a slightly lower rate of slow secondary hydrogenation reactions (7). In contrast, the olefin content decreased with increasing residence time, in spite of the concurrent increase in H_2O concentrations, because of a higher extent of α-olefin readsorption with increasing residence time (26). Similar trends were observed for higher hydrocarbons, as illustrated by the 1-octene/*n*-octane molar ratios shown as a function of the average water partial pressure in Fig. 5. These experiments also showed that water inhibits chain termination by hydrogen abstraction at internal positions in alkyl chains and secondary olefin isomerization reactions, as indicated by the observed increase in 1-pentene/2-pentene ratios with increasing water concentration (Table 1).

Similar experiments were carried out at 0.5 MPa and 473 K on 12.7 wt% Co/SiO_2 in order to determine whether these strong water effects were also observed at the lower pressures accessible in our infrared reactor cell. CO conversion and CH_4 and C_{5+} formation rates are shown in Fig. 6 as a function of the average H_2O partial pressure; these results confirmed that similar effects of H_2O are observed at

TABLE 1

Effect of Water Concentration on the Performance of the 12.7 wt% Co/SiO_2 Catalyst at 473 K, 2 MPa, and $H_2/CO = 2$

Space velocity ($cm^3/(g \cdot s)$)	Average H_2O pressure (MPa)	CO conversion (%)	CO conversion rate (h^{-1})	CH_4 formation rate (h^{-1})	C_{5+} formation rate (h^{-1})	CH_4 selectivity (%)	C_{5+} selectivity (%)	1-C_5H_{10}/*n*-C_5H_{12} ratio	1-C_8H_{16}/*n*-C_8H_{18} ratio	1-C_5H_{10}/2-C_5H_{10} ratio
0.28	0.11	28.8	30.1	1.98	26.54	6.6	88.3	1.23	0.29	15.8
0.18	0.22	48.8	34.0	1.79	30.64	5.3	90.2	1.29	0.35	14.8
0.56	0.04	12.6	26.3	1.98	22.77	7.5	86.5	1.81	0.56	33.5
0.86	0.03	8.4	26.4	2.07	22.67	7.8	86.0	2.08	0.72	36.2
0.86	0.24	11.5	36.1	1.77	32.56	4.9	90.1	2.58	1.57	86.6
0.86	0.46	17.6	55.2	2.03	50.55	3.7	91.6	2.76	1.85	144.4
0.86	0.87	20.9	65.5	1.83	60.43	2.8	92.2	2.89	2.13	114.6

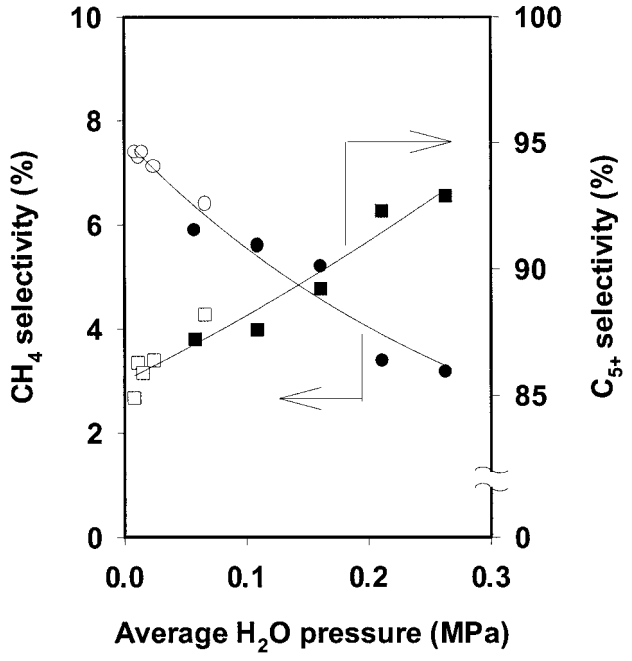

FIG. 7. CH_4 selectivities (○, ●) and C_{5+} selectivities (□, ■) as a function of the average water partial pressure on 12.7% Co/SiO_2 catalyst at 473 K, 0.5 MPa, $H_2/CO = 2$. (Open symbols) Space velocity runs; (filled symbols) water-addition runs.

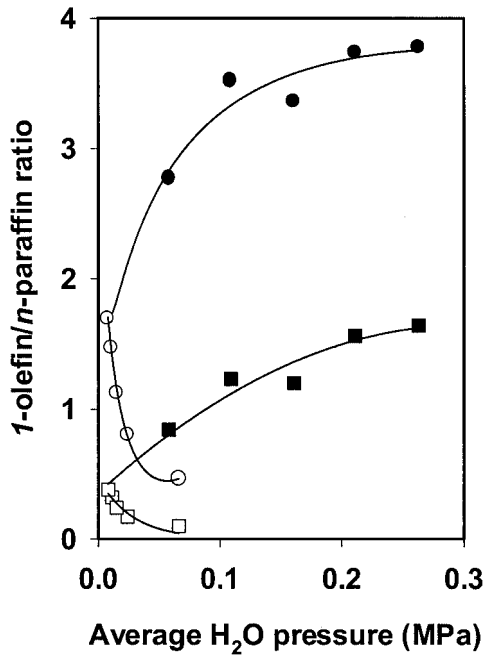

FIG. 8. 1-Pentene/*n*-pentane ratios (○, ●) and 1-octene/*n*-octane ratios (□, ■) as a function of the average water partial pressure on 12.7 wt% Co/SiO_2 catalyst at 473 K, 0.5 MPa, $H_2/CO = 2$. (Open symbols) Space velocity runs; (filled symbols) water-addition runs.

these lower synthesis gas pressures. As also found at higher pressures (Fig. 3), space velocity and water addition data lie along the same curve (Fig. 6). CH_4 selectivities decreased and C_{5+} selectivities increased with increasing water concentration also at these lower pressures (Fig. 7, Table 2) while the paraffin and internal olefin content in products concurrently decreased (Fig. 8, Table 2).

Distinct methanation and chain growth sites on Co surfaces and the selective titration of the former by H_2O have been proposed without evidence in order to explain the observed water effects on FTS selectivity (8). This proposal fails to explain the observed rate changes; moreover, it is not consistent with the finding that H_2O actually increases C_{5+} formation rates but leaves CH_4 formation rates largely unchanged (Fig. 3). Water inhibits olefin hydrogenation (27) and the termination of surface alkyl chains via addition of adsorbed hydrogen to form paraffins (7). Both of these effects are consistent with a decrease in the availability of hydrogen on active Co surfaces. Adsorbed hydrogen, however, is required also to form CH_x monomers involved in chain growth; thus, the concurrent increase in FTS reaction rates cannot be simply explained by lower

TABLE 2

Effect of Water Concentration on the Performance of the 12.7 wt% Co/SiO_2 Catalyst at 473 K, 0.5 MPa, and $H_2/CO = 2$

Space velocity ($cm^3/(g \cdot s)$)	Average H_2O pressure (MPa)	CO conversion (%)	CO conversion rate (h^{-1})	CH_4 formation rate (h^{-1})	C_{5+} formation rate (h^{-1})	CH_4 selectivity %	C_{5+} selectivity %	1-C_5H_{10}/*n*-C_5H_{12} ratio	1-C_8H_{16}/*n*-C_8H_{18} ratio	1-C_5H_{10}/2-C_5H_{10} ratio
0.08	0.07	56.8	16.9	1.08	14.91	6.4	88.2	0.46	0.10	2.1
0.17	0.02	26.7	16.8	1.19	14.52	7.1	86.4	0.80	0.17	3.8
0.25	0.02	18.2	16.6	1.23	14.26	7.4	85.9	1.12	0.24	5.4
0.35	0.01	13.1	16.8	1.23	14.50	7.3	86.3	1.47	0.32	7.3
0.50	0.01	9.8	17.8	1.32	15.11	7.4	84.9	1.69	0.38	8.4
0.50	0.06	10.2	18.5	1.09	16.13	5.9	87.2	2.77	0.84	19.5
0.50	0.11	11.4	20.8	1.16	18.22	5.6	87.6	3.52	1.23	34.4
0.50	0.16	13.5	24.6	1.28	21.94	5.2	89.2	3.36	1.20	31.0
0.50	0.21	14.1	25.7	0.87	23.72	3.4	92.3	3.74	1.56	38.1
0.50	0.26	13.9	25.3	0.81	23.50	3.2	92.9	3.78	1.64	41.0

concentrations of adsorbed hydrogen as H_2O concentrations increase.

Several plausible explanations for these H_2O effects on FTS reactions have been proposed (7). For example, an intrapellet water-rich phase, favored at high H_2O partial pressures, may be able to increase CO transport rates and also CO concentrations near intrapellet Co sites, because the solubility and diffusivity of CO is higher in water than in liquid hydrocarbons (28). Intrapellet CO concentration gradients would lead to lower FTS rates and lower C_{5+} and olefin selectivity; thus, an increase in CO diffusion rates would cause concomitant increases in CO conversion rates and C_{5+} and olefin selectivities, as observed experimentally with increasing H_2O partial pressure. Higher transport rates mediated by intrapellet aqueous or water-rich phase would also account for the unexplained effect of support structure on the magnitude of these rate enhancements (7) and for the contradictory effects of water on FTS rates in various studies. For example, the addition of water did not influence reaction rates on Co–Ru/ZrO_2/Aerosil (8) but led to lower rates on Co–Re/Al_2O_3 (5). Co/SiO_2 catalysts with larger pores showed marked rate enhancements with H_2O, while rates on Co supported on SiO_2 with smaller pores were unaffected (7).

H_2O could also influence FTS rates by increasing the intrinsic activity of exposed Co atoms (turnover rate) or the number of exposed Co surface atoms available for CO chemisorption and for monomer formation and chain growth. In the first case, H_2O may become involved in alternate CO activation pathways unavailable with dry synthesis gas reactants. We have probed the kinetic involvement of water in relevant elementary steps by measuring FTS reaction rates and selectivities using CO/H_2 and CO/D_2 mixtures and the resulting kinetic isotope effects as a function of water concentrations. Changes in kinetic isotope effects with increasing conversion and water concentrations would indicate the participation of water in FTS reaction steps unavailable in the absence of water. Water may be able to influence the number of exposed Co atoms by acting as a scavenger of unreactive carbon-containing species or their precursors, thus preserving a larger fraction of the initial number of Co surface atoms available during reaction. We discuss next our measurements of the kinetic isotope effects for FTS reactions on Co/SiO_2. Then, we explore the effects of water on the density of CO binding sites by collecting infrared spectra during FTS reactions using synthesis gas with and without added water.

Kinetic Isotope Effects in Fischer–Tropsch Synthesis

Kinetic isotope effects for CO conversion were obtained from the relative CO conversion rates using $CO/H_2/N_2$ and $CO/D_2/N_2$ reactant mixtures and for the formation of each product from their corresponding rates of formation from these two reactant mixtures. CO conversion and C_{5+} formation rates are shown as a function of average water partial pressure (H_2O or D_2O) in Figs. 9a and 9b, respectively, for CO/H_2 and CO/D_2 mixtures on 21.9 wt% Co/SiO_2. The water partial pressure was varied by changing the extent of CO conversion through changes in reactant space velocity. For both CO/H_2 and CO/D_2 reactants, CO conversion (Fig. 9a) and C_{5+} formation rates (Fig. 9b) increased with increasing CO conversion, as a result of the concomitant increase in water concentration. Kinetic isotope effects, defined as the ratio of the rates with CO/H_2 and CO/D_2 mixtures (r_H/r_D), are shown in Fig. 10 for CO conversion, CH_4 formation, and C_{5+} formation rates as a function of average H_2O partial pressure. These data are presented at two CO conversion levels in Table 3 together with 1-pentene/*n*-pentane and l-nonene/*n*-nonane ratios for the two reactant mixtures. The KIE values in Fig. 10 were calculated by taking the corresponding experimental rates (or olefin/paraffin ratios) for CO/H_2 reactants and dividing each one by the interpolated value of the rate at the same water partial pressure for CO/D_2 reactants. The rates reported in Table 3 are actual KIE ratios at the corresponding conversions prevalent with H_2 and D_2 coreactants. The KIE values for CO consumption and for C_{5+} formation were ~0.8 and they were not influenced by the average water partial pressure in the reactor. These values are very similar to those reported previously (29); their constant values with changes in water concentration suggest that kinetically relevant pathways in FTS reactions were unchanged as water concentrations varied over the experimental range.

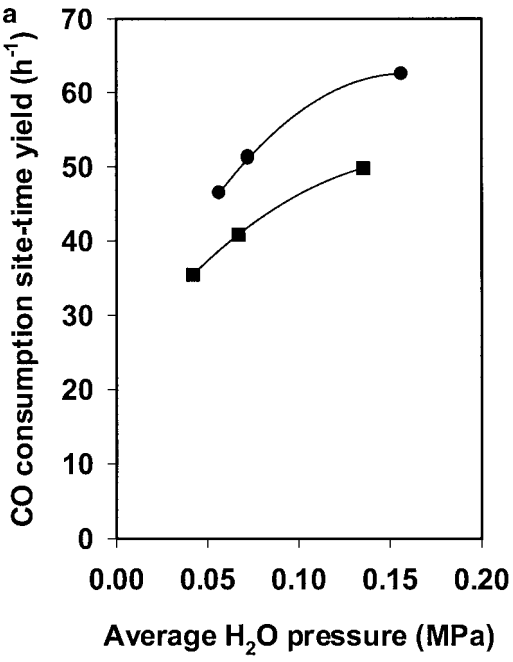

FIG. 9a. CO consumption site-time yield as a function of the average H_2O partial pressure on the 21.9 wt% Co/SiO_2 catalyst: ●, D_2; ■, H_2; 473 K; 2 MPa; $H_2/CO = D_2/CO = 2$.

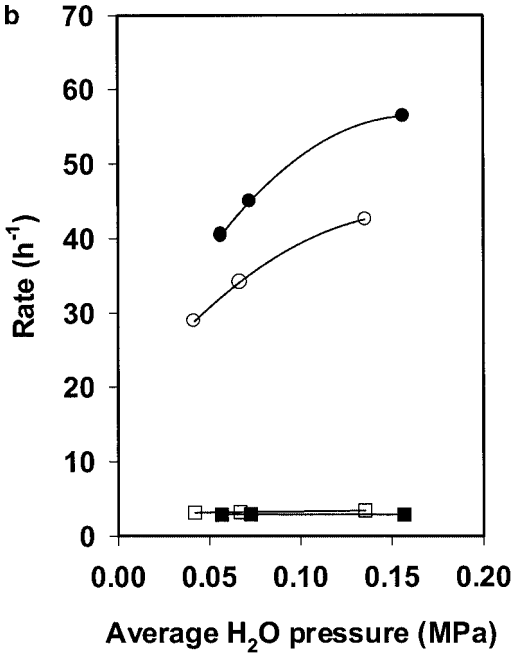

FIG. 9b. C_{5+} (●, ○) and methane (■, □) formation rates as a function of the average H_2O partial pressure on the 21.9 wt% Co/SiO_2 catalyst. (Filled symbols) D_2; (open symbols) H_2, 473 K, 2 MPa, $H_2/CO = D_2/CO = 2$.

In this range, CO conversion and C_{5+} formation rates both increased by a factor of ∼1.5. It is interesting that KIE values for CH_4 formation were larger than one (1.1–1.2) and increased slightly with increasing H_2O concentration

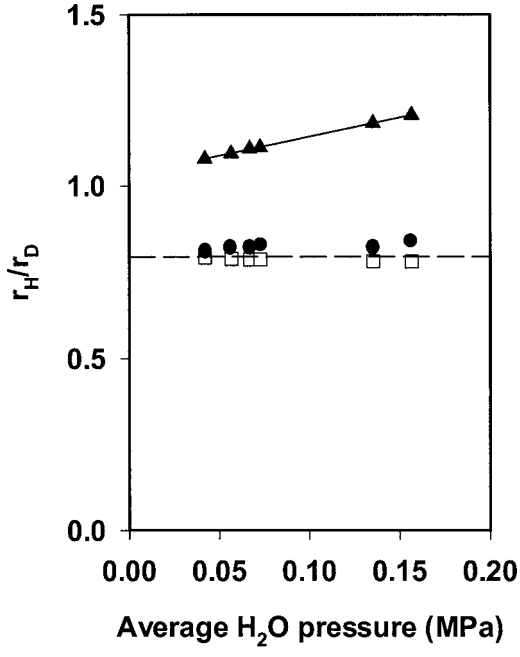

FIG. 10. Isotope effect (r_H/r_D) as a function of the average H_2O partial pressure on the 21.9 wt% catalyst: ●, CO consumption; ▲, CH_4 formation; □, C_{5+} formation; 473 K; 2 MPa; $H_2/CO = D_2/CO = 2$.

TABLE 3

FTS Rate and Selectivity Data on the 21.9 wt% Co/SiO_2 Catalyst for Reactions with CO/H_2 and CO/D_2 Mixtures (473 K, 2 MPa, $H_2/CO = D_2/CO = 2$)

FTS parameters	19–20% conversion			35–39% conversion		
	H_2	D_2	KIE	H_2	D_2	KIE
CO consumption rate (h^{-1})	40.8	51.2	0.80	49.8	62.5	0.80
CH_4/CD_4 formation rate (h^{-1})	3.2	2.9	1.10	3.4	2.9	1.17
C_2–C_4 formation rate (h^{-1})	3.5	3.3	1.06	3.9	3.2	1.21
C_{5+} formation rate (h^{-1})	34.1	45.0	0.76	42.5	56.4	0.75
$1\text{-}C_5H_{10}/n\text{-}C_5H_{12}$	2.0	2.0	1.00	1.7	1.8	0.94
$1\text{-}C_9H_{18}/n\text{-}C_9H_{20}$	0.5	0.6	0.83	0.3	0.5	0.60

(Fig. 9b), even though CH_4 formation rates were not influenced by H_2O concentrations. These normal isotope effects are in contrast to the inverse isotope effects measured for CO conversion and C_{5+} formation, the underlying basis for which remains speculative at this time. Olefin/paraffin ratios were very similar with CO/H_2 and CO/D_2 mixtures for C_5 hydrocarbons and the corresponding KIE values were independent of water partial pressure. For higher hydrocarbons (e.g., C_9), olefin-to-paraffin ratios were slightly higher for CO/D_2 mixtures than for CO/H_2 mixtures, and these differences increased with increasing H_2O partial pressure (Table 3).

If hydrogenation of C* to form a C_1^* monomer were the kinetically relevant step (16, 30), FTS rates with CO/H_2 and CO/D_2 would be given, respectively, by

$$r_H = k_H\theta_H\theta_C,$$
$$r_D = k_D\theta_D\theta_C,$$

with the kinetics isotope effect then given by

$$\frac{r_H}{r_D} = \frac{k_H\theta_H}{k_D\theta_D},$$

where k_i are the rate constants and θ_i is the fractional coverage of each individual species i (H_2 or D_2) during reaction. When H_2 and CO adsorption steps are quasi-equilibrated, the fractional coverage, θ_i, is a function of their respective adsorption equilibrium constants, K_i, and partial pressures, P_i; i.e.,

$$\theta_H = \frac{\left(K_{H_2}P_{H_2}\right)^{0.5}}{1 + \left(K_{H_2}P_{H_2}\right)^{0.5} + K_{CO}P_{CO}},$$

where K_{CO} and P_{CO} are the adsorption equilibrium constant and the partial pressure for CO, respectively.

When the hydrogen coverage is small compared with that of carbon-containing intermediates, $(K_{H_2}P_{H_2})^{0.5} \ll K_{CO}P_{CO}$

and the above equation becomes

$$\theta_H = \frac{(K_{H_2} P_{H_2})^{0.5}}{1 + K_{CO} P_{CO}}.$$

Hence, $\frac{\theta_H}{\theta_D} = [\frac{K_{H_2} P_{H_2}}{K_{D_2} P_{D_2}}]^{0.5} = [\frac{K_{H_2}}{K_{D_2}}]^{0.5}$ for the similar P_{H_2} and P_{D_2} in our case. The overall isotope effect then becomes a combination of kinetic and thermodynamic isotope effects according to the expression

$$\frac{r_H}{r_D} = \frac{k_H}{k_D} \left[\frac{K_{H_2}}{K_{D_2}}\right]^{0.5}.$$

For this case, in which C–H bond formation is the kinetically relevant step, we expect an inverse kinetic isotope effect ($k_H/k_D < 1$) although this depends on the relative strengths of the H and D bonds with the surface and with carbon in CH_x species and on the extent to which these two bonds have broken or formed, respectively, in the activated complex involved in this elementary step. A similar derivation for the case of the hydrogenation of a CH^* species to form CH_2 as the kinetically relevant step leads to a kinetic isotope effect given by

$$\frac{r_H}{r_D} = \frac{k_H}{k_D} \left[\frac{K_{H_2}}{K_{D_2}}\right]^{1.0},$$

with a correspondingly stronger thermodynamic contribution to the observed kinetic isotope effects. The thermodynamic component of the isotope effect depends on the relative chemisorption enthalpies of D_2 and H_2 on Co surfaces. Previous studies have indicated that chemisorption of D_2 is preferred over that of H_2 on Ni and Fe catalysts (31). Similar data are not available on Co surfaces, but we expect inverse thermodynamic isotope effects for hydrogen chemisorption similar to those on Ni and Fe. The overall isotope effect for CO conversion and for C_{5+} formation is ~0.8 in our case (Fig. 10), suggesting that thermodynamic factors and the net formation of a C–H bond in the activated complex for the formation of either CH or CH_2 influence the measured overall isotope effects. A more rigorous analysis of these kinetic isotope effects requires molecular simulations of proposed elementary steps and their respective kinetic isotope effects, an approach that is beyond the scope of the present study.

Irrespective of the detailed mechanistic interpretation of the observed isotope effects, a change in their magnitude would be expected if water introduced kinetically relevant steps that overcame kinetic bottlenecks responsible for the reaction rates observed with dry H_2/CO feeds. Instead, kinetic isotope effects for CO consumption and for C_{5+} formation rates are unaffected by water concentration, which rules out such changes in kinetically relevant steps as the mechanistic basis for the higher rates observed with increasing water concentration. These results provide experimental evidence against the direct involvement of water in kinetically relevant FTS reaction steps or in the thermodynamic properties of Co surfaces for CO adsorption. We consider next the alternate possibility that water leads to a higher density of accessible active sites, via scavenging any deactivating sites that form during the initial stages of H_2/CO reactions. In doing so, we measure the number of CO binding sites as a function of water concentration using infrared spectroscopy during FTS reactions on Co/SiO_2 catalysts.

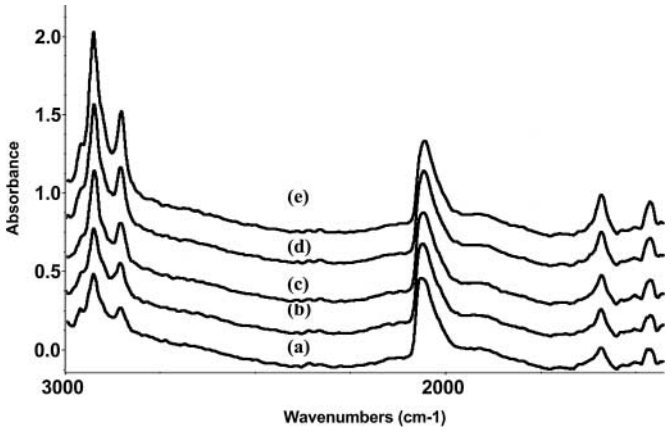

FIG. 11. Evolution of FTIR spectra as a function of time under reaction conditions on the 12.7 wt% Co/SiO_2 catalyst at 473 K and 0.5 MPa ($H_2/CO = 2$, 3.6×10^3 cm^3/h flow rate). (a) 1 min, (b) 10 min, (c) 20 min, (d) 40 min, and (e) 66 min.

Infrared Spectra during Fischer–Tropsch Synthesis on Co/SiO₂

In situ infrared spectra were collected at 473 K and 0.5 MPa ($H_2/CO = 2$); representative spectra are shown in Fig. 11 as a function of time on stream for 12.7 wt% Co/SiO_2. Several strong bands for adsorbed species were detected and their frequencies and assignments reflect those reported previously on Ru and Co catalysts (18–21). The band at 1590 cm^{-1} (symmetric –OCO– stretches) and a doublet, at 1390 (–CH deformation modes) and 1377 cm^{-1} (antisymmetric –OCO– stretching vibrations, obscured by intense hydroxyl SiO_2 bands), arise from formate groups adsorbed on SiO_2. The 2067-cm^{-1} band corresponds to linearly adsorbed CO on Co (18, 19). This band initially weakens and shifts slightly (to 2057 cm^{-1}) with time on stream; it reaches a steady-state intensity in ~1 h. Two intense bands, at 2927 and 2855 cm^{-1}, are assigned to symmetric and antisymmetric C–H vibrations in methylene groups (18, 19), while the band at 1450 cm^{-1} arises from C–H bending modes in $–CH_2$ groups. The weak shoulder at 2959 cm^{-1} is typical of symmetric C–H stretches of $–CH_3$ groups; the antisymmetric modes are often masked by intense $–CH_2$ stretching bands (19–21). Figure 11 shows that the bands for methyl and methylene groups become more intense with time on stream, suggesting that they arise from growing

chains or adsorbed hydrocarbons formed from H_2/CO reactants. Previous reports have suggested that these bands are associated with growing chains, because they are not observed when fresh samples are exposed to typical Fischer-Tropsch synthesis products (19). A weak band was also detected at ~1900 cm^{-1} in our samples; this band is characteristic of bridged –CO– stretching vibrations on metal surfaces.

Isotopic switch studies have shown than active Co and Ru surfaces are predominately covered by adsorbed CO during FTS, even near ambient pressures (26). As a result, the intensity of the band for adsorbed CO for a given sample is proportional to the number of exposed Co atoms available for FTS turnovers. After steady-state spectra were collected at 473 K and 0.5 MPa, H_2O (0.05 MPa) was added and infrared spectra were collected until all CO absorption bands reached again a constant intensity. The H_2O concentration was then increased to 0.1 MPa and infrared spectra were collected until the intensity of all bands again reached constant values. Then, H_2O was removed from the synthesis gas stream and infrared spectra were again collected until steady-state intensities were achieved. The steady-state spectra for the initial and final dry synthesis gas experiments and for these two water concentrations are shown in Fig. 12. The addition of water led to a slight initial decrease in the frequency of the adsorbed CO band (from ~2070 to ~2050 cm^{-1}) and to the appearance of an intense band at 1628 cm^{-1}, which corresponds to deformation modes in molecularly adsorbed water (19–22). This band was also detected on pure SiO_2 when water was added to the synthesis gas stream. The CO bands did not revert to their original frequency upon water removal, but adsorbed water bands disappeared gradually after H_2O was removed from the synthesis gas stream. After these experiments, the sample temperature was decreased to 453 K, spectra were collected, and H_2O (0.05 MPa) was added. The spectra and conclusions were similar to those obtained at 473 K.

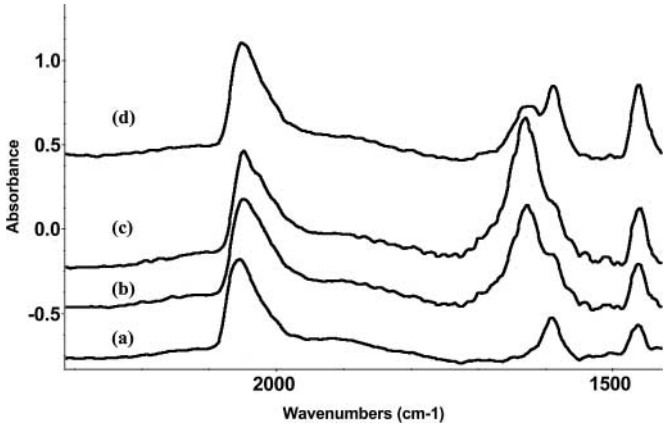

FIG. 12. Effect of water addition on steady-state FTIR spectra under reaction conditions on the 12.7 wt% Co/SiO_2 catalyst (473 K, 0.5 MPa, $H_2/CO = 2$, 3.6×10^3 cm^3/h flow rate). (a) No water added; (b) 0.05 MPa H_2O; (c) 0.1 MPa H_2O; (d) H_2O stopped.

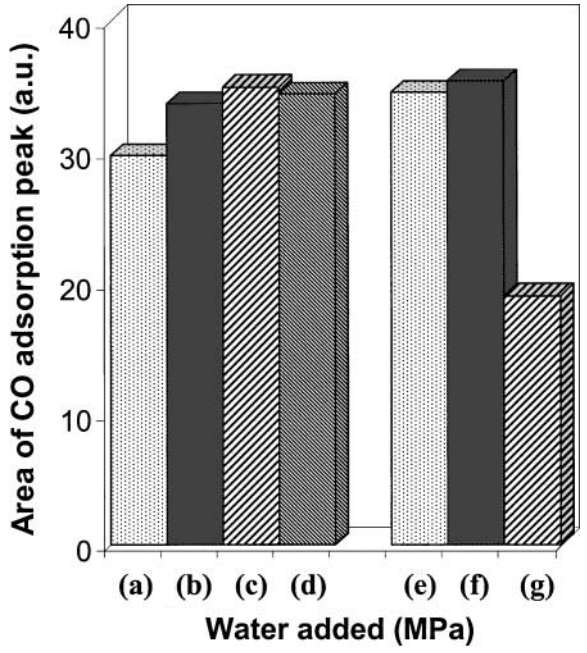

FIG. 13. Effect of added water on the area of the CO adsorption peak at (a) 473 K, no water, (b) 473 K, 0.05 MPa H_2O, (c) 473 K, 0.1 MPa H_2O, (d) 473 K, H_2O stopped, (e) 453 K, no water, (f) 453 K, 0.05 MPa H_2O, and (g) 453 K, 0.1 MPa H_2O (0.5 MPa, $H_2/CO = 2$, 3.6×10^3 cm^3/h flow rate).

The areas under the infrared CO band are shown in Fig. 13 for the experiments described above. At 473 K, the presence of H_2O (0.05 MPa) increased the initial CO band intensity by ~15% and then by another 5% when the H_2O pressure was increased to 0.1 MPa. These changes in intensity were smaller than the changes of 16 and 30% in CO conversion rates (from ~16.0 h^{-1} at very low CO conversions to 18.5 and 20.8 h^{-1} with 0.05 and 0.1 MPa H_2O for CO consumption) and in C_{5+} formation rates observed when these water concentrations are added to the synthesis gas stream at 473 K and 0.5 MPa. Clearly, these rate enhancements do not reflect a higher steady-state density of exposed Co sites when H_2O is present. The observed rate enhancements were fully reversed upon water removal, but the CO infrared band did not return to its initial intensity when H_2O was removed from the synthesis gas stream at 473 K (Fig. 13). Hence, the small initial increase in CO band intensity observed upon H_2O addition does not appear to be related to the increase in FTS rate observed upon water addition. This band also did not change in intensity when 0.05 MPa H_2O was again added during subsequent experiments at 453 K. The initial changes in the CO band intensities appear to reflect a gradual approach to a steady-state Co surface, which contains a slightly smaller number of CO adsorption sites than does the fresh Co/SiO_2 sample. After these initial changes, our *in situ* infrared spectroscopy studies showed that the intensity of the adsorbed CO bands

were unchanged over long periods of contact with synthesis gas (>24 h), suggesting that CO transport restrictions, which would have led to the depletion of CO from intrapellet regions as pores filled with liquid products over several hours, are not important during these FTS experiments.

High H_2O concentrations (0.25 MPa) led to irreversible changes in the intensity of the adsorbed CO infrared band. The infrared spectra before H_2O addition were not recovered upon removal of water from the synthesis gas stream. Catalytic reaction rates at 0.5 MPa H_2/CO and 0.25 MPa H_2O also showed a gradual and irreversible decrease with increasing time of exposure to this reactant mixture. These high H_2O/H_2 ratios appear to lead to the oxidation of active Co surfaces and to the formation of adsorbed oxygen islands, which do not readily react with adsorbed hydrogen at the same rate as isolated adsorbed oxygen species formed in CO dissociation reactions. At H_2O/H_2 ratios below 0.8, the availability of CO binding sites appears to be unaffected by changes in H_2O partial pressures in the range that leads to strong enhancements of CO conversion and C_{5+} formation rates during Fischer–Tropsch synthesis.

These studies appear to rule out a scavenging effect of H_2O on inactive adsorbed species or their precursors. They also cast some doubt on the possible role of water in the removal of any prevalent CO transport restrictions, because such effects would have led to reversible effects of water on intrapellet CO concentrations and thus on the intensity of infrared bands for adsorbed CO. While inhibition of FTS rates caused by transport require significant diffusional limitations because of the typical negative order of FTS rates in CO, selectivity effects are quite marked even for small intrapellet CO concentration gradients. Any such small gradients may not be detectable because of the near monolayer coverages of CO at typical CO partial pressures. Thus, we cannot rule out based on the results presented here any such diffusional constraints as the basis for the observed effects of H_2O on selectivity, but we can conclude that the corresponding effects of water on rates are negligible.

Based on our results, it appears that water does not influence the number of CO binding sites available during reaction or change the chemical characteristics of such binding sites. The nature, reactivity, and number of active carbon species during FTS reactions on Co surfaces may be influenced in subtle ways by the presence of varying amounts of H_2O, without any accompanying changes in the number of exposed Co sites available for CO adsorption or in the way that such active species react with adsorbed hydrogen (or deuterium) atoms in the kinetically relevant monomer formation steps. Previous studies have proposed the presence of active carbon species for CO hydrogenation reactions on Co and Ru based on measurements of isotopic and chemical transients (26, 32). A shift in reactivity or density for the active monomer precursors can lead not only to higher rates of chain growth, but also to a higher probability of chain growth, without any significant changes in chain termination probability. Detailed investigations of these phenomena remain essential in our efforts to understand these important effects of water on FTS reactions catalyzed by Co surfaces. This study represents a starting point for such investigations by providing kinetic and spectroscopic evidence that rules out some of plausible explanations provided in earlier studies.

CONCLUSIONS

Indigenous or added H_2O led to marked increases in CO conversion and C_{5+} formation rates and in the average molecular weight and olefin contents of FTS reaction products. Kinetic isotope effects (r_H/r_D) were measured during FTS in order to probe the possible participation of water in kinetically relevant steps during FTS on Co surfaces. Kinetic isotope effects for CO conversion and C_{5+} formation were less than unity, suggesting a contribution of hydrogen adsorption–desorption thermodynamics and of C–H bond formation in kinetically relevant steps. These kinetic isotope effects were unaffected by water concentrations that led to significant changes in CO conversion and C_{5+} formation rates, indicating that the presence of H or D in water does not influence the number and the reactivity of the reaction intermediates involved in these kinetically relevant steps. *In situ* infrared spectroscopy was used in order to characterize the various adsorbed species present during FTS reactions and the chemical nature of metal surfaces on Co crystallites supported on SiO_2 at various water concentrations. The density of available Co surface atoms (obtained from the intensity of adsorbed CO infrared bands) and the structure of adsorbed CO (obtained from the frequency of CO infrared bands) were not affected by water concentrations in a range leading to significant enhancements in CO conversion rates and C_{5+} and olefin selectivities. These infrared studies also detected the surface oxidation of SiO_2-supported Co crystallites at H_2O/H_2 ratios greater than 0.8 at a reaction temperature of 473 K. We conclude that H_2O effects do not arise from new pathways introduced by water, by scavenging effects of H_2O on the concentration of site-blocking unreactive intermediates, or by removing significant CO transport restrictions. As a result, we are left with only the possibility that water influences the relative concentration of the active and inactive forms of carbon, present at low concentrations on Co surfaces. The mechanism by which such effects occur without measurable (H_2O/D_2O) kinetic isotope effects remains unclear.

ACKNOWLEDGMENTS

The authors acknowledge the financial support provided by the U.S. Department of Energy (DE-FC26-98FT40308). The authors also acknowledge helpful technical discussions with Professor Charles A. Mims of the

University of Toronto and Drs. Gabor A. Kiss and Stuart L. Soled of ExxonMobil Research and Engineering Co.

REFERENCES

1. Fischer, F., and Tropsch, H., *Brennstoff-Chem.* **7**, 97 (1926).
2. Anderson, R. B., *in* "Catalysis" (P. H. Emmett, Ed.), Vol. 4, p. 29. Van Nostrand–Reinhold, New York, 1956.
3. Storch, H. H., Golumbic, N., and Anderson, R. B., "The Fischer-Tropsch and Related Syntheses." Wiley, New York, 1951; Anderson, R. B., "The Fischer-Tropsch Synthesis." Wiley, New York, 1984.
4. Dry, M. E., *in* "Catalysis—Science and Technology" (J. R. Anderson and M. Boudart, Eds.), Vol. 1, p. 160. Springer-Verlag, New York, 1981.
5. Schanke, D., Hilmen, A. M., Bergene, E., Kinnari, K., Rytter, E., Adnanes, E., and Holmen, A., *Catal. Lett.* **34**, 269 (1995).
6. Kim, C. J., U.S. Patent 5,227,407 (1993), assigned to Exxon. Res. Eng. Co.
7. Iglesia, E., *Appl. Catal. A* **161**, 59 (1997).
8. Schulz, H., van Steen, E., and Claeys, M., *Stud. Surf. Sci. Catal.* **81**, 455 (1994).
9. Van Berge, P. J., van de Loosdrecht, J., Barradas, S., and van der Kraan, A. M., *Catal. Today* **58**, 321 (2000).
10. Gottschalk, F. M., Copperthwaite, R. G., van der Riet, M., and Hutchings, G. J., *Appl. Catal.* A **38**, 103 (1998).
11. Schulz, H., Claeys, M., and Harms, S., *Stud. Surf. Sci. Catal.* **107**, 193 (1997).
12. Eur. Patent Appls. 201,557 (1983), assigned to Shell.
13. Rothaemel, M., Hanssen, K. F., Blekkan, E. A., Schanke, D., and Holmen, A., *Catal. Today* **38**, 79 (1997).
14. Hanssen, K. F., Blekkan, E. A., Schanke, D., and Holmen, A., *Stud. Surf. Sci. Catal.* **109**, 193 (1997).
15. Tauster, S. J., and Fung, S. C., *J. Catal.* **55**, 29 (1978).
16. van Steen, E., and Schulz, H., *Appl. Catal. A* **186**, 309 (1999).
17. Claeys, M., and van Steen, E., *Catal. Today* **71**, 419 (2002).
18. Dalla Betta, R. A., and Shelef, M., *J. Catal.* **48**, 111 (1977).
19. Ekerdt, J. G., and Bell, A. T., *J. Catal.* **58**, 170 (1979).
20. King, D. L., *J. Catal.* **61**, 77 (1980).
21. Kadinov, G., Bonev, Ch., Todorova, S., and Palazov, A., *J. Chem. Soc. Faraday Trans.* **94**, 3027 (1998).
22. Rygh, L. E. S., Ellestad, O. H., Klæboe, P., and Nielsen, C. J., *Phys. Chem. Chem. Phys.* **2**, 1835 (2000).
23. Winslow, P., and Bell, A. T., *J. Catal.* **94**, 385 (1985).
24. Zowtiak, J. M., Weatherbee, G. D., and Bartholomew, C. H., *J. Catal.* **82**, 230 (1983); **83**, 107 (1983).
25. Li, S., Krishnamoorthy, S., Li, A., Meitzner, G. D., and Iglesia, E., *J. Catal.* **206**, 202 (2002).
26. Kellner, C. S., and Bell, A. T., *J. Catal.* **67**, 175 (1981).
27. Iglesia, E., Reyes, S. C., Madon, R. J., and Soled, S. L., *Adv. Catal.* **39**, 221 (1993).
28. Reid, R. C., Prausnitz, J. M., and Sherwood, T. K., "The Properties of Gases and Liquids." McGraw–Hill, New York, 1977.
29. Sakharoff, M. M., and Dokukina, E. S., *Kinet. Katal.* **2**, 710 (1961).
30. Raje, A. P., and Davis, B. H., *in* "Catalysis" (J. J. Spivey, Ed.), Vol. 12, p. 65. Royal Soc. of Chemistry, Cambridge, U.K., 1996.
31. Biloen, P., Helle, H., and Sachtler, W., *J. Catal.* **44**, 439 (1979).
32. Bertole, C. J., Mims, C. A., Kiss, G., and Joshi, P., *Stud. Surf. Sci. Catal.* **136**, 375 (2001).